MESON PRODUCTION STUDIED WITH THE GEM DETECTOR*

H. MACHNER

Institut für Kernphysik, Forschungszentrum Jülich, Jülich, Germany

representing the GEM collaboration

A. Budzanowski[4], P. Cloth[1], H. Dąbrowski[4], A. Djaloeis[1], M. Drochner[3,5], V. Drüke[1], J. Ernst[11], W. Erven[5], D. Filges[1], D. Frekers[9], D. Grzonka[1], J. Holzer[5], St. Igel[1], R. Jahn[11], L. Jarczyk[2], K . Kilian[1], J. Konin[8], T. Kutsarova[10], M. Kystrin[2], B. J. Lieb[7], H. Machner[1], W. Meiling[3], H. P. Morsch[1], Ch. Nake[1], H. S. Plendl[6], D. Protic[1], G. Riepe[1], E. Roderburg[1], P. von Rossen[1], R. Schwierz[3], J. Smyrski[2], A. Strzałkowski[2], P. Turek[1], K. H. Watzlawik[1], K. Zwoll[5]

1. Institut für Kernphysik, Forschungszentrum Jülich, Jülich, Germany
2. Physics Institute, Jagellonian University, Cracow, Poland
3. Institut für Kernphysik, T. U. Dresden, Dresden, Germany
4. Institute of Nuclear Physics, Cracow, Poland
5. Zentralinstitut für Elektronik, Forschungszentrum Jülich, Jülich, Germany
6. Florida State University, Tallahassee, Florida, USA
7. George Mason University, Fairfax, Virginia, USA
8. NIKEF K, Amsterdam, Netherlands
9. Institut für Kernphysik der Universität Münster, Münster, Germany
10. Institute of Nuclear Research and Nuclear Energy, Bulgarian Academy of Sciences, Sofia, Bulgaria
11. Institut für Kernphysik, Universität Bonn, Bonn, Germany

(Received August 31, 1993)

The GEM detector system is described. Meson production near threshold in $p+d$ reactions leading to two- and three-body final states is discussed. Details of the search for bound states in the cases of π^-'s and η's are given.

PACS numbers: 29.40. Gx

---

* Presented at the Meson–Nucleus Interactions Conference, Cracow, Poland, May 14–19, 1993.

1. Introduction

The advent of cooled beams from accelerators like the Indiana Cooler, the CELSIUS ring in Uppsala and COSY in Jülich has revitalized the investigation of light meson production close to threshold. In this contribution we will focus on the experimental program of the GEM detector system presently assembled at COSY. We will discuss first the details of the GEM detector system. It will be shown that this system is ideally suited for the study of reactions in which light mesons are produced not too f ar above threshold. Of special interest is the $p + d \rightarrow {}^3\mathrm{He}$+meson reaction following the pioneering work performed at SATURNE in Saclay [1, 2, 3]. In contrast to all previous we will make use of a 4π-detector. In addition the unbound states of the nucleons in the final state are presently also of interest.

The formation of pionic atoms in low-lying states in heavier nuclei is a long standing problem. Already in 1954 Deser *et al.* [4] pointed out that even the knowledge of the algebraic sign of the level shift in pionic $1s$ states of light nuclei would be of value. With shift we denote in the following the shift of the level due to the strong interaction when compared to the pure Coulomb interaction. Only half a year later Brückner [5] introduced an additional broadening of such levels due to strong absorption. At the same time Kisslinger [6] determined an optical model from the scattering of pions on ${}^{12}\mathrm{C}$. These three quantities, level width, shift and optical potential, are still the main ingredients in the study of pionic atoms, although, the theory of pion-nucleus interactions is nowadays much more elaborate. A more complete description can by found in Refs [7, 8].

On the experimental side we are still dealing with only two observables for each level with given principal and angular momentum quantum numbers: the width and the shift of the level. The 1s state is in this respect of special interest. Because in this state the overlap between the pion density and the nuclear density is maximal, the observables of this state should be most sensitive to the short-range strong interaction. The classical method of pionic atom formation by π^--absorption was recently extended up to ${}^{27}\mathrm{Al}$ and ${}^{28}\mathrm{Si}$ [9]. These measurements yielded an improved parameterization of the optical potential. This improved parameterization predicts a saturation of the widths. As an example the width $\Gamma(1s)$ for ${}^{40}\mathrm{Ca}$ is predicted to be 82 keV and 94 keV for the standard and the improved parameterization, respectively. These numbers are 474 keV and 63 keV for ${}^{208}\mathrm{Pb}$.

Pionic atoms in the 1s state for nuclei heavier than ${}^3\mathrm{He}$ are bound only via the Coulomb force while the strong interaction is repulsive. On the contrary the existence of strongly bound η mesic atoms was predicted [10] if the $N^*(1535)$ plays a dominant role.

2. The GEM detector

The GEM detector is a hybrid system consisting of GErmanium wall plus Magnetic spectrometer. The spectrometer is a remodeled version of the previous BIG KARL spectrometer. In order to allow for ray tracing in the x- and y-direction its previous two entrance quadrupole magnets were replaced by three high field quadrupole magnets. These magnets have a larger opening than the previous ones giving a larger acceptance of the spectrometer. The first dipole magnet has a new side yoke. It allows now, together with a window in a new vacuum chamber, for exits of the primary beam. This works if the $B\rho$-values of the primary beam and the particles to be measured differ by factors of two to three and the spectrometer is at zero degrees (see Fig. 1). In addition to BIG KARL II a stack of position-sensitive germanium detectors will be used (see Fig. 2), the germanium wall which will enlarge the spatial acceptance of the magnetic spectrometer. These two detector elements together cover an solid angle of 560 mrad. They will allow direction measurement and energy measurement each to better than 10^{-3} as we will discuss below.

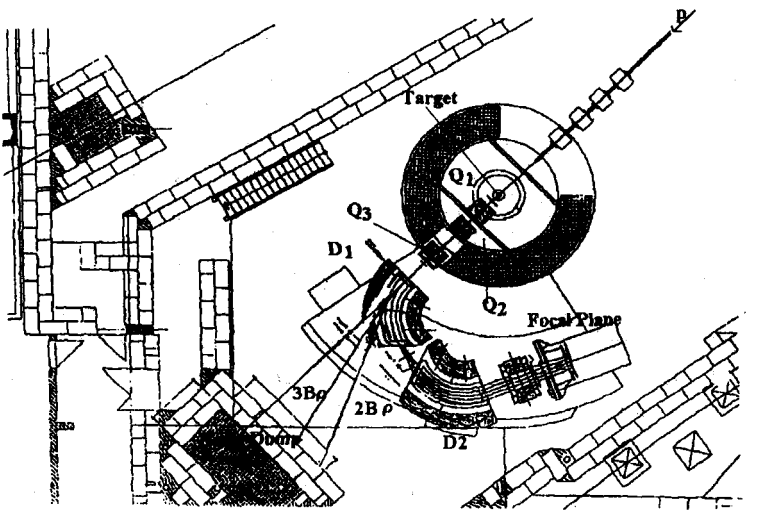

Fig. 1. View of the target area with the remodeled magnetic spectrometer BIG KARL II. Indicated are the new three entrance quadrupole magnets and the two dipole magnets. The first dipole has exits for the primary beam. The two limiting cases of factors two and three with respect to the detected particles are indicated. The primary beam is dumped in a shielded piece of iron of $1\,m^3$ volume.

To allow for precise emission angle measurements the small beam spot of COSY (0.6 mm in diameter or less) together with a small emittance is

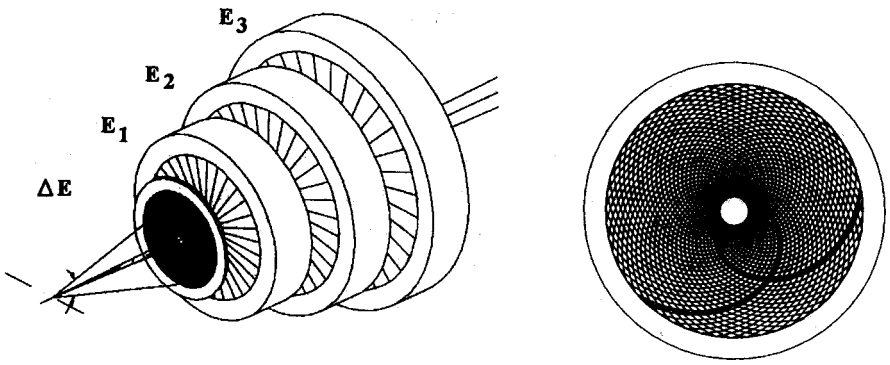

Fig. 2. Perspective view of the Ge-wall. The first detector has 200 Archimedes' spirals on the front side and 200 on the rear side but with opposite orientation (quirl detector). Thus 40000 pixels are defined. The following diodes have pie structures with 32 slices each. All diodes are transition detectors. Right: Enlarged view of the quirl. Out of the 200 spirals only 50 are shown for clarity. The definition of a pixel as crossing between two spirals is indicated.

essential. In order to not spoil these advantages thin targets are necessary. For solid targets this is not a problem. In the case of liquid deuterium we will make use of a 2 mm thin target with extremely thin walls [11]. The distance from target to Ge-Wall is optimized with respect to energy and solid angle acceptances and will be 60 mm (see Fig. [3]). The hole in the middle of the Ge-Wall serves as an exit for the primary beam. ^{3}He-particles scattered into this region will be measured by BIG KARL II, which detects the outgoing particles within ± 28 mrad with respect to the forward direction with similar resolution. The particle trajectories going into that angular range will be measured with two sets of multi-wire drift chambers in the focal plane. These detectors will be followed by a plastic trigger hodoscope which will also allow for time of flight measurements to reduce background. Use of a 4π detector around the target to detect additional decay products is foreseen.

3. Bremsstrahlung

When a 470 MeV proton interacts with deuterium several processes will occur with cross sections compiled in Fig. 4. The strongest channel is fragmentation, followed by elastic scattering. Then pion production takes place on a millibarn level for the many-body final states and a few tens of μbarns for the two-body final states. The pure electromagnetic bremsstrahlung process takes place only on a 500 nb level. It is, therefore, evident that this is the most complicated process to be measured. To examine the bremsstrahlung process the detector has to allow a precise measurement of the invariant

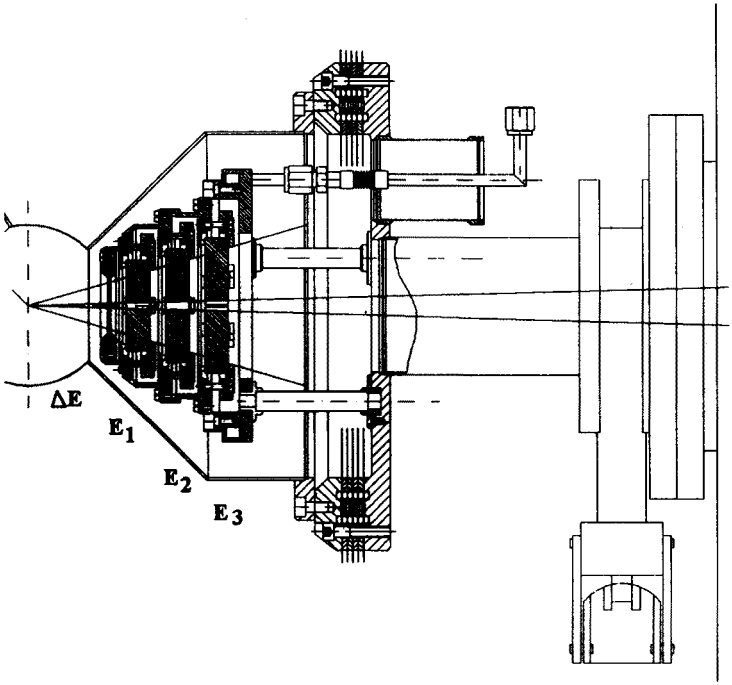

Fig. 3. Side view of the Ge-Wall.

mass of the unobserved particle to distinguish between the γ and the π^0 from the kinematically not too different ^{3}He+π^0 channel, which is 20 times more frequent [13]. In order to distinguish between processes, Cameron *et al.* [14] employed an additional photon detector. However, these authors point out that normalization problems exist in bremsstrahlung measurements when they compare their results with previous data.

The kinematics of the reaction is shown in the top part of Fig. 5 as a polar diagram, *i.e.* the kinematical loci are plotted as function of the momenta parallel to the beam axis and the momenta perpendicular to it. In addition the acceptances of the two detector components are also shown. A Δ-E detector of 800 μm thickness was assumed. A projectile momentum of 900 MeV/c is the limiting momentum for GEM acting as a 4π detector. At the momentum of 600 MeV/c, which is just below the π^0 threshold, a part of the events will not reach the E_1- detector.

High precision absolute data will allow to perform serious tests of the principle of detailed balance by comparison with data from the inverse reaction, photofission of ^{3}He. The additional measurement of the analyzing power will allow investigation of small amplitudes.

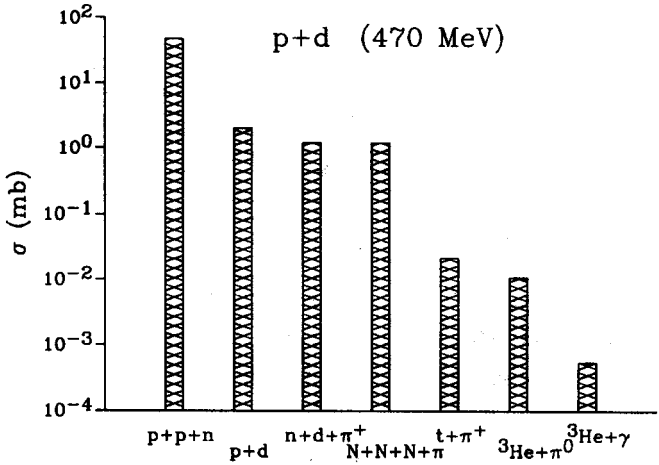

Fig. 4. Cross sections for the indicated reaction channels ordered according to decreasing probability. The data are from Dollhopf *et al.* and Carrol *et al.* In addition we have assumed isospin symmetry.

4. Pion production

The next most likely reaction channels shown in Fig. 4 are pion production associated by fusion into $A = 3$ systems. The kinematics of both processes is also shown in Fig. 5. It is evident that GEM is a 4π detection device for energies from threshold up to 500 MeV corresponding to $\eta = p^{\pi}_{max}/m_{\pi} = 1.6$. Why is this energy regime of interest? First of all because of the poverty of cross section measurements. In Fig. 6 we show the excitation function of $^3\mathrm{He}+\pi^0$ measurements. The values close to threshold were given by Pickar *et al.* [15], the other data were obtained by fitting Legendre polynomial L_l to the data $d\sigma(\theta)/d\Omega = \sum_{l=0}^{l=2} p_l L_l(\theta)$ and $\sigma = 4\pi p_0$. The data shown are transformed assuming isospin symmetry and time reversal invariance and are from Refs [12, 16–20]. We have taken only such data into account which span large angular ranges and consist at least of five data points. There is obviously a gap between $0.2 < \eta < 0.8$ where no data exist. In the region above $\eta = 1$ the data do not follow one unique curve. The one shown is generated by Pickar et al. which is the momentum dependence of the $p + n \rightarrow d + \pi^0$ cross section divided by 80. Although the general trend is accounted for by this curve serious discrepancies exist especially close to threshold. There are no data available around the maximum. This maximum in the total cross section should not be mixed up with the one seen in backward angle production [21] at $\eta \approx 1.9$ and explained by Kilian and Nann [22] as a result of the underlying kinematics if a two- step process is the dominating reaction channel.

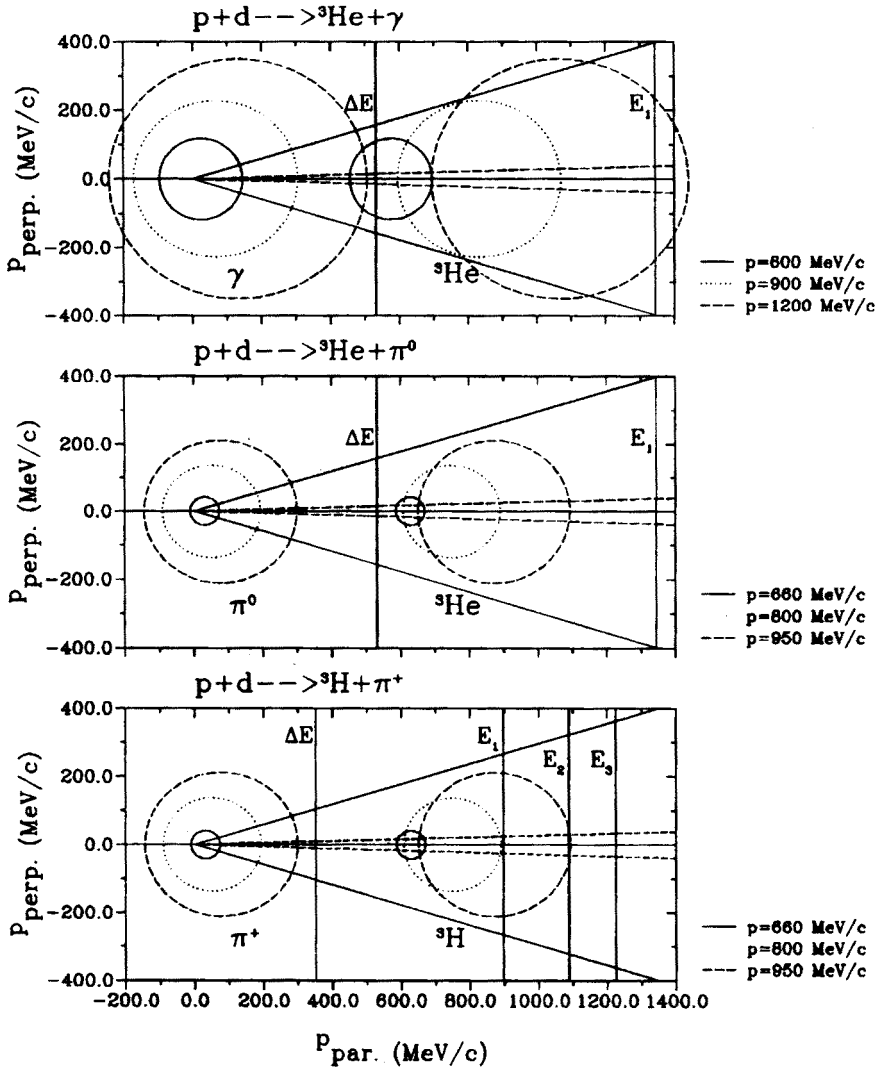

Fig. 5. Polar diagram of the kinematical loci for the indicated reactions shown as function of the momenta parallel and perpendicular to the beam direction. Calculations are for the beam momenta given in the figure. The spatial acceptances of the magnetic spectrometer and the Ge-wall as well as the energy acceptance of the components of the latter device are indicated by dashed and solid lines, respectively.

Also the differential data show discrepancies between different measurements especially at backward angles. Some of the existing data sets could

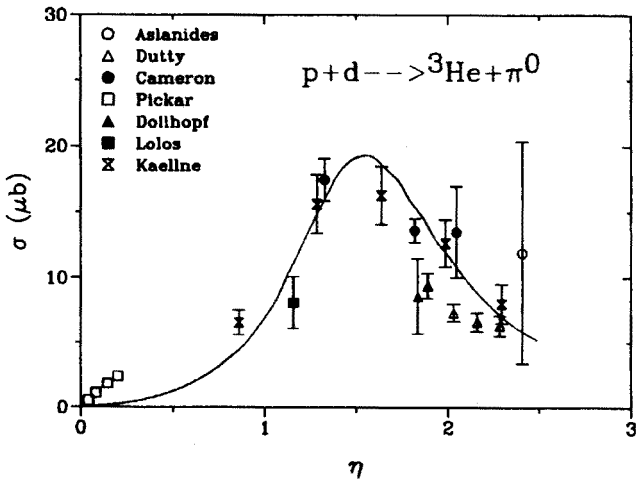

Fig. 6. Excitation function of the indicated reaction. The data are extracted total cross sections from the angular distributions given in the indicated references. The solid curve is the momentum dependence of the $p + n \rightarrow d + \pi^0$ reaction divided by 80 as extracted by Pickar *et al.*

not even be fitted by series of Legendre polynomials. We, therefore, plan to measure such cross sections with high precision. Again, polarization will help to entangle the reaction mechanism. Also the question of isospin invariance of the strong interaction in the pion sector is of importance [23], as is the question of time reversal invariance.

5. Eta-production

5.1. The p + d reaction

The next heavier meson is the η with mass 548 MeV which has a heavier sister, the η' at 958 MeV. Comparisons of the matrix elements of the production cross sections with those for π^0 production as function of the four-momentum transfer $t = (p_p - p_d)^2$ in the

$$p + d \rightarrow {}^3\mathrm{He} + \eta \text{ or } \eta' \qquad (1)$$

reactions should allow insight into the constituent quark composition. Again, GEM can be used as a 4π-detector which is also suited to measure analyzing powers. Also the question of the reaction mechanism can be addressed. One possibility for the η is the production of a N^* resonance which then can decay into a nucleon and the meson. In Fig. 7 the probability is shown for N^*-resonances to decay into this channel. Obviously, the $N^*(1535)$ dominates the cross section close to threshold. The solid line indicates the limit of GEM as a 4π-detector. Another possible mechanism could again be a

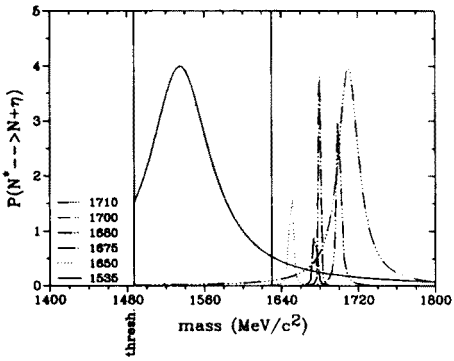

Fig. 7. Positions and widths of N^* resonances which decay into $N + \eta$. Also shown is the mass range of the present experiment (vertical lines).

two-step process [22] with first the formation of a π which then in a second scattering produces the η. A maximum close to threshold should occur in that case due to the underlying kinematics.

A preliminary Monte Carlo simulation of the $p+d \rightarrow {}^3\mathrm{He}+\eta$ experiment has been made with the code MC3 [24] assuming phase space distributions of the produced mesons. The detector was simply represented by a mesh. We have assumed systematic errors in the angle measurement from target thickness, a beam radius of $0.3\,mm$, and a mean emittance of 1πmm mrad. In Fig. 8 the reconstructed missing mass squared is shown for an energy close to threshold. As background reaction in the range of interest we have assumed two pion production. The ratio between total background and η cross section was estimated according to the measurements by Banaigs *et al.* [1]. From simulations employing an uncooled beam the missing mass distribution for the η broadens leading to a less favorable ratio between signal to background. But even for this case the experiment seems to be feasible.

The cross section for the $p + d \rightarrow p + d + \eta$ reaction can be estimated to be $800\,\mu b$ from the corresponding π^0 reaction and from deducing the matrix elements from the $p+d \rightarrow {}^3\mathrm{He}+$neutral meson reactions. If this large cross section substantiates, even rare decay studies will become feasible with COSY.

For the $p + d \rightarrow p + d + \eta$ reaction a somewhat different experimental setup is required due to the different kinematics. In Fig. 10 the envelopes of the kinematical loci for protons and deuterons for two different beam momenta are shown. The real kinematical loci will be inside the ellipses shown depending on the four-momentum vector of the η. Also shown are the acceptances of the Ge-Wall and the magnetic spectrometer as dashed lines. Evidently, the detector acceptance is too narrow for the higher beam momentum which corresponds to the recoil-free case for the reaction leading to ${}^3\mathrm{He}+\eta$.

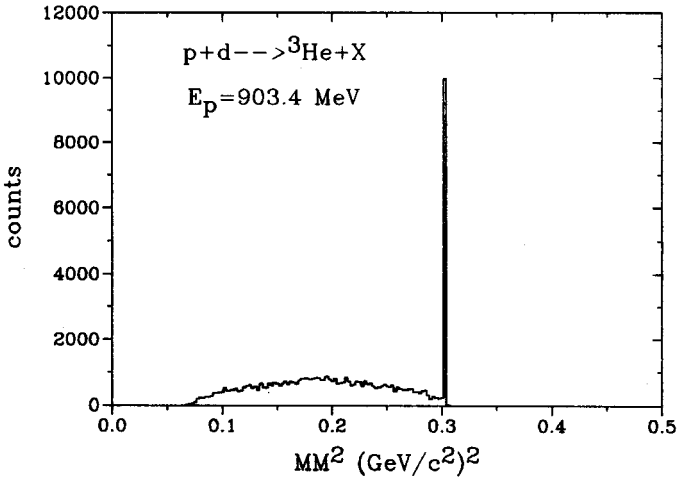

Fig. 8. Missing mass as obtained by Monte Carlo simulation of the reaction shown for a bombarding energy of 903 MeV.

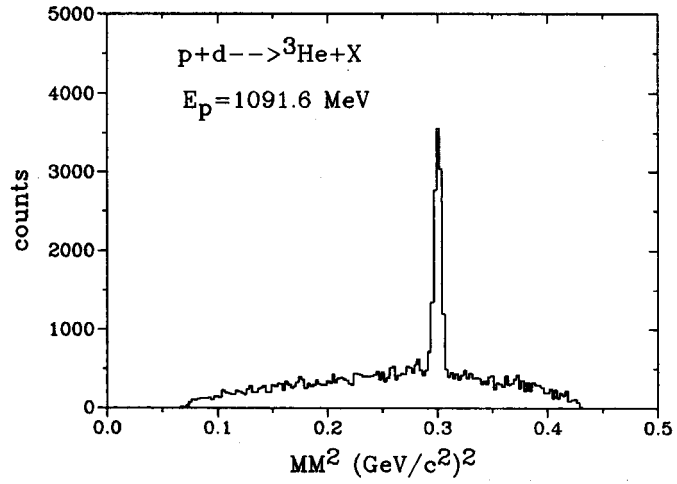

Fig. 9. Same as previous figure but for 1092 MeV bombarding energy.

We, therefore, propose to amalgamate a part of the Ge-Wall with the TOF-detector for the present reaction and for momenta which cannot be detected by the above discussed apparatus. For identification of the directions of the protons and deuterons the ΔE germanium detector will be used. It will also deliver ΔE information. This detector will be directly followed by the last diode with the largest diameter of all diodes in the Ge-Wall which will then cover the whole solid angle. The distance from target to the first detector is for this geometry 28 mm. The corresponding proton and

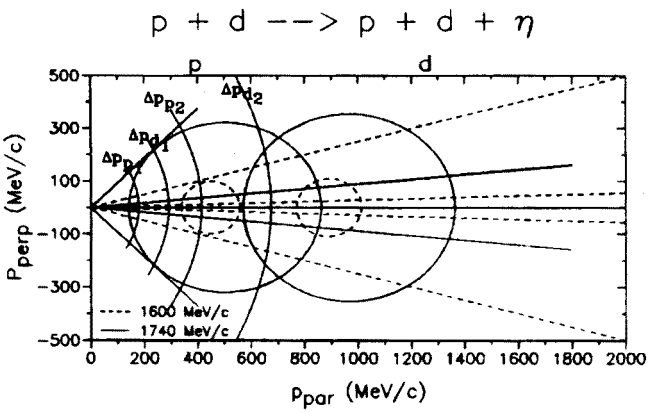

Fig. 10. Polar diagram of the kinematical ellipses for protons and deuterons from the indicated reaction. All curves and lines for a proton beam momentum of 1600 MeV/c are broken, those for 1740 MeV/c are solidly drawn. The ellipses are the envelopes of the kinematical loci which depend on the momenta of the η mesons. The lines show the acceptances of the Ge-Wall for the two geometries discussed. Particles in the narrow cone will be detected by the magnetic spectrometer for the low bombarding momentum and by the TOF detector for the high momentum. The momentum ranges of the two germanium diodes foreseen are indicated for protons and deuterons as well and indicated by the corresponding indices.

deuteron momenta for these two germanium detectors are also shown in the figure. While at the lower bombarding momentum a portion of the protons will be stopped completely in the solid state detector, the higher proton momenta as well as the deuteron momenta are too high to be stopped in these diodes. However, these high energy particles will deliver energy loss signals sufficiently large to identify the particle type. If these measurements do not suffice to derive the total energy, an additional flight time measurement with a following scintillator as start detector and the front of the TOF detector as stop detector 2.5 m downstream will provide the additional information needed. Although this reaction channel cannot be measured with the same accuracy and only over a more limited momentum range than the ^{3}He channel, it is expected to provide valuable information on the reaction mechanism.

5.2. The p+A reaction

It seems natural to compare η production with π^0 production. Close to threshold the latter is dominated by S-wave production. The cross sections for some reactions are given in Table I.

TABLE I

Comparison of neutral meson production cross sections near threshold

Reaction	$\sigma(\pi^0)(\mu b)$	Ref.	$\sigma(\eta)(\mu b)$	Ref.
$p+p \rightarrow p+p+X^0$	3.8	[25]	1	[27]
$n+p \rightarrow d+X^0$	10	[26]	100	[29]
$p+d \rightarrow {}^3\mathrm{He}+X^0$	2	[15]	0.4	[28]

Whereas η production is by a factor of 4 smaller than π^0 production it is a factor of ten larger in the deuteron formation. This sheds some light on the importance of the neutron in the η production process. It is, therefore, worthwhile to measure production yields also on heavier nuclei. One interesting case would be the $p+{}^6\mathrm{Li} \rightarrow {}^7\mathrm{Be}+\eta$ reaction because the target has a cluster substructure making the reaction almost like reaction (1). A thinner ΔE-detector has to be used to measure the recoiling ^{7}Be. Again GEM is a 4π-detector and with a few mg/cm^2 thick target the resolution is good enough to resolve low-lying states in the recoiling ^{7}Be which is not the case in the measurements performed so far [30]. In these measurements the η's were detected by their weak decay into two photons. Comparison of these data with the presently proposed ones should enable one to deduce information on the absorption process of η's in nuclei.

6. Bound states

6.1. Pionic atoms

If the meson-nucleus interaction is attractive, bound states (*i.e.* mesic atoms) can be formed. For a study of the strong interaction, low-lying states of pionic atoms are of interest. The interaction in the atomic $1s$ state is attractive for nuclei up to ^{3}He and repulsive for heavier ones. Consequently, only π^--atoms can be studied for heavier systems because in these cases binding comes from the Coulomb force. The classical method of π^--absorption can not be applied because the widths of states for nuclei heavier than ^{28}Si is in the order of 50 keV and cannot be distinguished from background in γ-spectra. Therefore, a different experimental technique is required. In hadronic production it was first pointed out by Ericson and Kilian [31] that recoil free production as it is used in the production of hypernuclei is also possible for light mesons. We follow this conjecture since it will maximize the yield of bound pions. In Fig. 11 we show the excitation function for the formation of pionic atoms via the elementary process

$$p+n \rightarrow p+p+\pi^- \qquad (2)$$

with three different choices of the neutron momentum. The momentum 0 MeV/c corresponds to the elementary process where favoring recoil free kinematics really pays. For a typical Fermi momentum of 75 MeV/c, which corresponds to a valence neutron, the effect is still there although weaker than for the free neutron. For a Fermi momentum of 150 MeV/c, which corresponds to a more deeply bound neutron, the effect of recoil free kinematics is almost gone. It should be noted that the present calculations show the effect of subthreshold production in the case of bound neutrons due to the Fermi motion.

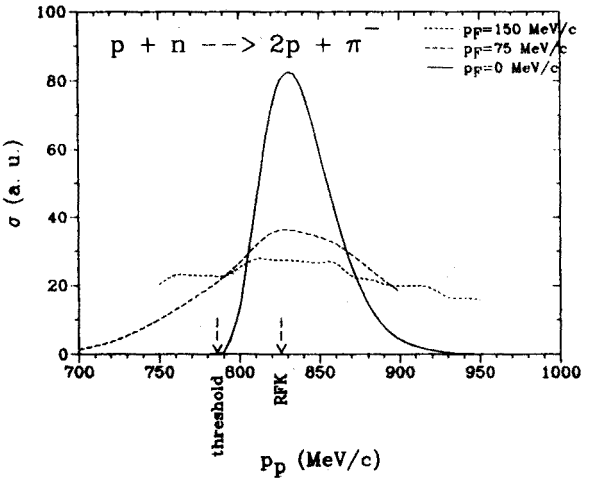

Fig. 11. Excitation function for the formation of a pionic atom in a 1s state for the indicated reaction. The (Fermi-) momentum of the neutron p_F, is given as capture to the appropriate curve. Structures are due to limited statistics in the Monte Carlo method.

From these calculations we conclude that recoil free kinematics favors the formation of bound pion-nucleus states in the case of weakly bound neutrons or, in other words, on nuclei where the last shell is fully occupied. This is again as in hyper-nuclear spectroscopy. Target nuclei to be chosen under these constraints are ^{28}Si, ^{40,44,48}Ca, and ^{208}Pb. All these nuclei have the first excited state more than 2 MeV above the ground state and, therefore, will not have a mixing between nuclear and pionic atomic excitations. With the first target we can prove the method by comparison with existing data, continuing then to unknown cases. Of special interest will be the investigation of the calcium isotopes. Although the pionic atom will live some time, it will finally decay by annihilation. This can happen in a naive picture only on a deuteron or two protons. A possible neutron skin on the calcium surface for the heavier isotopes will lead to a longer life

time corresponding to a smaller width. Such a prediction was made in the context of super-heavy nuclei by Friedman and Soff [32].

There is of course also a physical "background" due to a $(p, 2p)$ reaction with a many-body final state. The background was estimated by calculations in the framework of the exciton coalescence model [33, 34] to be 100 μb in the detector acceptance, which will be given below, in an energy bin of 300 keV for each proton. The expected instrumental mass resolution will be of the order of 100 keV. This has to be compared with 70 nb for the formation of a pionic atom in the ground state. The detector was designed so that all this cross section will be detected. We, therefore, expect the background to be of the same order of magnitude as the spectral line.

GEM is for the bound system again a 4π-detector. Its missing mass resolution will allow the measurement of the level shift for all nuclei of interest and also the width for the heavier nuclei. It will allow to distinguish between the standard and modified optical potential mentioned above.

6.2. Eta-mesic nuclei

Similar to the pionic atom case, one can produce the η without recoil in the $p+d \rightarrow {}^3\mathrm{He}+\eta$ reaction. This enables us to search for bound or resonant η-nuclear states. For such states to exist, the η-nucleus interaction has to be sufficiently attractive. Theoretical studies by Haider and Liu [10] indicate such a binding for nuclei heavier than ^{12}C. Furthermore, the lifetime of the η in nuclei should not be too short. Calculations [10] yielded 3. 6 MeV for ^{12}C up to 11 MeV for ^{208}Pb. Since in nuclei there is a lot of quasi-deuterons the detection of ^{3}He should give a clean signal of a bound state. In order to have an additional information, one can detect the reaction products after the η-absorption as well. The strongest channel will be $\eta + N \rightarrow N^* \rightarrow N + \pi$. This process will lead to a nucleon and a pion being emitted back to back with 467 MeV/c momentum.

7. Conclusion

We have presented a detector system with high granularity and good energy resolution. It is near threshold a 4π-detector in reactions with meson production. The main goals of the experiments proposed with this system are the study of the reaction mechanism, the importance of the quark content of the mesons and the interactions of mesons with nuclei at small momenta. Also the question of isospin invariance and time reversal invariance in meson production can be addressed. The data emerging from GEM are expected to have factors of 30 better statistics than existing data, thus allowing stringent tests of these symmetries.

REFERENCES

[1] J. Banaigs *et al.*, *Nucl. Phys.* **B67**, 1 (1973).

[2] J. Berger *et al.*, *Phys. Rev. Lett.* **61**, 922 (1988).

[3] F. Plouin, Production and Decay of Light Mesons (Proc. of a Saturne Workshop), ed. P. Fleury, p. 114, World Scientific, Singapore 1988; A. Boudard, *Nucl. Phys.* **A508**, 229c (1990).

[4] S. Deser *et al.*, *Phys. Rev.* **96**, 774 (1954).

[5] K.A. Brueckner, *Phys. Rev.* **98**, 769 (1955).

[6] L.S. Kisslinger, *Phys. Rev.* **98**, 761 (1955).

[7] D.S. Koltun, *Advances in Nuclear Physics*, Vol. 3, Plenum Press 1969.

[8] F. Scheck, *Leptons, Hadrons and Nuclei*, North Holland Publ., Amsterdam 1983.

[9] J. Koonin, C.T.A.M. De Laat, A. Taal, J.H. Koch, *Nucl. Phys.* **A519**, 773 (1990).

[10] Q. Haider, L.C. Liu, *Phys. Lett.* **B172**, 257 (1986).

[11] Ch. Nake, K. Kilian, H. Machner, P. Turek, contribution to this conference.

[12] W. Dollhopf, C. Lunke, C.F. Perdrisat, W.K. Roberts, P. Kitching, W.C. Olsen, J.R. Priest, Nucl. Phys. **A217**, 381 (1973).

[13] J. Carroll, D.H. Fredrickson, M. Goitain, B. Macdonald, V. Prez-Mendez, A. Stezt, C.A. Heusch, R.V. Kline, K.T. McDonald, *Nucl. Phys.* **A305**, 502 (1978).

[14] J.M. Cameron, P. Kitching, W.J. McDonald, J. Pasos, J. Soukup, J. Thekkumthala, H.S. Wilson, R. Abegg, D.A. Hutcheon, C.A. Miller, A.W. Stetz, I.J. van Heerden, *Nucl. Phys.* **A424**, 549 (1984).

[15] M.A. Pickar, A.D. Bacher, H.O. Meyer, R.E. Pollock, G.T. Emery, *Phys. Rev.* **C46**, 397 (1992).

[16] E. Aslanides, R. Bertini, O. Bing, F. Brochard, Ph. Gorodetzky, F. Hibou, T.S. Bauer, R. Beurtey, A. Boudard, G. Bruge, H. Catz, A. Chaumeaux, P. Couvert, L. Bimbot, Y. Le Bornec, B. Tatischeff, *Phys. Rev. Lett.* **39**, 1654 (1977).

[17] J. Källne, J.E. Bolger, M.J. Devereaux, S.L. Verbeck, *Phys. Rev.* **C24**, 1102 (1981).

[18] G.J. Lolos, E.L. Mathie, G. Jones, E.G. Auld, G. Giles, B. McParland, P.L. Walden, W. Ziegler, W.R. Falk, *Nucl. Phys.* **A386**, 477 (1982).

[19] J.M. Cameron, P. Kitching, J. Pasos, J. Thekkumthala, R. Abegg, D.A. Hutcheon, C.A. Miller, S.A. Elbakr, A.H. Hussein, *Nucl. Phys.* **A472**, 718 (1987).

[20] W. Dutty, J. Franz, E. Rössle, H. Schmitt, L. Schmitt, Proceedings of the Tenth International IUPAP Conference on Few Body Problems in Physics, Karlsruhe 1983, Vol. II, North Holland, Amsterdam 1984, p. 235; E. Rössle, Priv. Communications.

[21] C. Kerboul, A. Boudard, L. Antonuk, J. Arvieux, J. Berger, R. Bertini, M. Boivin, J.M. Durand, A. Stetz, J. Tinsley, J. Yonnet, *Phys. Lett.* **B181**, 28 (1986).

[22] K. Kilian, H. Nann, Proc. Conf. on Particle Production Near Threshold, Sept. 1990, Nashville, Indiana, AIP Conf. Proc 221, Particle and Fields Series 41, American Institute of Pysics, NY, 1991, p. 185.
[23] G.A. Miller, B.M.K. Nefkens, I. Slaus, *Phys. Rep.* **194**, 1 (1990).
[24] D. Filges, G. Sterzenbach, Monte Carlo Code MC3 (unpublished).
[25] H.O. Meyer, C. Horowitz, H. Nann, P.V. Pancella, S.F. Pate, R.E. Pollock, B. von Przewowski, T. Rinckel, M.A. Ross, F. Sperisen, *Nucl. Phys.* **A 539**, 633 (1992).
[26] D.A. Hutcheon, E. Korkmaz, G.A. Moz, R. Abegg, N.E. Davison, G.W.R. Edwards, L.G. Greeniaus, D. Mack, C.A. Miller, W.C. Olsen, I.J. van Heerden, Ye Yanlin, *Phys. Rev. Lett.* **64**, 176 (1990).
[27] A.M. Bergdolt *et al.*, to be published.
[28] R.S. Kessler, Ph. D. Thesis, UCLA, 1992, and to be published.
[29] B.M.K. Nefkens, Proceedings 105 International WE-Heraeus-Seminar on Hadronic Processes at Small Angles in Storage Rings, Bad Honnef 1993, Konferenzen des Forschungszentrums Jülich, **12**, 73 (1993).
[30] E. Scomparin, E. Chiavassa, G. Dellacasa, N. De Marco, F. Ferrero, P. Guaita, A. Musso, A. Piccotti, E. Vercellin, M. Gallio, R. Bertini, J.M. Durand, F. Brochard, P. Fassnacht, *J. Phys. G* **19**, L51 (1993).
[31] T.E.O. Ericson, K. Kilian in: Proceedings of the International Conference on Particle and Nuclei (PANIC-84), Heidelberg 1984, Book of abstracts, p. h9.
[32] E. Friedman, G. Soff, *J. Phys.G* **11**, L37 (1985).
[33] H. Machner, *Phys. Rev.* **C 29**, 109 (1984).
[34] H. Machner *et al.*, *Phys. Lett.* **128B**, 39 (1984).